Nonresonant Multiphoton Ionization of Stark Decelerated Molecules by Femtosecond Laser Pulses

Congsen Meng(孟从森)[1*], Zhihui Lü(吕治辉)[1], Xiaowei Wang(王小伟)[1], Dongwen Zhang(张栋文)[1], Zengxiu Zhao(赵增秀)[1], and Jianmin Yuan(袁建民)[1,2]

[1]*Department of Physics, National University of Defense Technology, Changsha 410073, China*
[2]*Department of Physics, Graduate School of China Academy of Engineering Physics, Beijing 100193, China*

(Received 17 August 2022; accepted manuscript online 23 September 2022)

Nonresonant multiphoton ionization by femtosecond laser pulses can be applied to any molecule virtually, thereby greatly enhancing the scope of Stark decelerated molecules. For comparison, we detect decelerated and trapped ammonia molecules using two different schemes: (i) nonresonant multiphoton ionization using intense femtosecond (fs) pulses in the near infrared, and (ii) resonance-enhanced multiphoton ionization using nanosecond (ns) pulses from a tunable UV laser. The observed number of ions per shot for both schemes is similar. The fs laser detection scheme suffers from an increased background, which can be effectively eliminated by subsequent mass and velocity selection. To determine the detection volume of the ns laser detection scheme, we present measurements in which the decelerated ammonia molecules are bunched to a packet with a longitudinal spread well below ∼100 μm. It is concluded that the detection volume for the ns laser detection scheme is 1.5–2 times larger than that of the fs laser detection scheme.

DOI: 10.1088/0256-307X/39/11/113701

Stark deceleration is proven to be one of the successful techniques for producing cold molecules.[1–6] In previous experiments on Stark deceleration, the conventional detection method is to utilize a nanosecond (ns) laser via resonance enhanced multiphoton ionization (REMPI) or laser induced fluorescence, where the availability of suitable transitions is a prerequisite. As the scope of Stark decelerated molecules expands, a more general detection method for cold and trapped poly-atomic molecules is quite desirable. Owing to the rapid development of laser technology during the last decades, amplified femtosecond laser systems produce focused laser intensities well over $10^{14}\,\mathrm{W/cm^2}$, corresponding to electric fields comparable to, or larger than, the atomic Coulomb fields that bind matter together.[7–10] This implies that virtually any atom or molecule will be ionized in laser focus, thus potentially providing a very general and sensitive detection method for atoms and molecules. The obvious downside of this nonresonant detection method is that it lacks state specificity which has thus far limited its use in molecular beam experiments. However, in Stark deceleration experiments, rotational cooling in the supersonic expansion combined with state selection in the Stark decelerator provides a pure sample in the rotational ground state. With the help of velocity map imaging and mass selection, unwanted signals from thermal gas in the vacuum chamber can be greatly suppressed. Another major advantage of femtosecond (fs) laser detection is that the well-defined detection volume allows an accurate determination of the density of the molecules in the beam. For multiphoton ionization, if only ions are collected from the central portion of the laser focus, where the laser beam is effectively parallel, the ion yield will vary as a function of the peak intensity in a simple way. This allows a direct measurement of ionization efficiencies, and can lead to absolute densities with few assumptions.[11] We have used this technique to determine the number of trapped methyl fluoride molecules before.[12]

In this work, we use an fs laser to detect Stark decelerated ammonia molecules and compare it to the conventional detection method that employs resonant multiphoton ionization by UV laser light from an ns dye laser.[13,14] The experiments described here are performed in a vertical molecular beam machine (see Fig. 1) that was previously used to decelerate and trap ammonia[15–17] and methyl fluoride molecules.[12] In brief, a mixture of 5% ammonia (NH_3) molecules in xenon is released into vacuum using a pulsed valve (Jordan valve) at a 10 Hz repetition rate. Ammonia molecules in the $|J, MK\rangle = |1, -1\rangle$ state are decelerated to 90–150 m/s using a conventional Stark decelerator consisting of 101 pairs of electrodes to which voltages of +10 kV and −10 kV are applied. A traveling wave decelerator, mounted 24 mm above the last electrode pair of the first decelerator, consists of a series of 336 rings to which oscillating voltages of ±5 kV are applied. By modulating the voltages sinusoidally in time, ammonia molecules inside the trap can be guided, decelerated and trapped.[18,19] The molecules are ionized 40 mm above the traveling-wave decelerator using light from either an fs or ns laser. The fs laser system consists of a titanium-sapphire oscillator (Spectra-Physics, Tsunami) and a chirped regenerative amplifier (Spectra-Physics, Spitfire Pro). The fundamental laser output at 800 nm (2 mJ per pulse, 1 kHz repetition rate, $\tau = 150$ fs) is focused using a lens with a 500 mm focal length, given a peak intensity of above $10^{14}\,\mathrm{W/cm^2}$. The ns laser system consists of a dye laser (Sirah) pumped by an Nd:YAG laser (Spectra Physics, Quanta-Ray). The output of the dye laser is doubled in a KD*P crystal yielding ∼10 mJ in a 5 ns pulse, which is focused using a lens with a focal length of 500 mm. The frequency of the laser

*Corresponding author. Email: mengcongsen08@nudt.edu.cn
© 2022 Chinese Physical Society and IOP Publishing Ltd

is resonant with the $\tilde{X}(1) \rightarrow \tilde{B}(3), {}^{r}S1_1^-$ transition around 161 nm. From the previous studies,[13,14] it was found that (2+1) REMPI via the $\tilde{B}$-state is the most efficient detection scheme for ammonia using ns lasers. While going to higher vibrational levels of the $\tilde{B}$-state, NH_3 predissociates more rapidly, but the dyes used in generating the tunable light become more efficient at the necessary wavelengths. We choose the $\nu_2 = 3$ as a compromise between the two. With the used laser power, a 500 mm lens gives us an optimal signal; focusing the laser more tightly results only in broadening the spectral lines to several wavenumbers. The lenses used to focus the fs and ns laser pulses are mounted on motorized translation stages that allow the position of the laser foci to be optimized in three directions. The laser-produced ions are mass-selectively detected using a double micro channel plate (MCP) mounted in front of a fast response ($1/e$ time ~10 ns) phosphor screen (Photonis P-47 MgO). The light of the phosphor screen is imaged onto a CCD camera and monitored by a photo multiplier tube. By setting the voltages of the ion lenses correctly, ions with the same initial transverse velocity are focused at the same position on the detector [velocity map imaging (VMI)[20]]. A mask on the back side of the phosphor screen is used to collect light originating from molecules with a small transverse velocity.[21] In this way, we can discriminate the signal of slow molecules from thermal background molecules.[22]

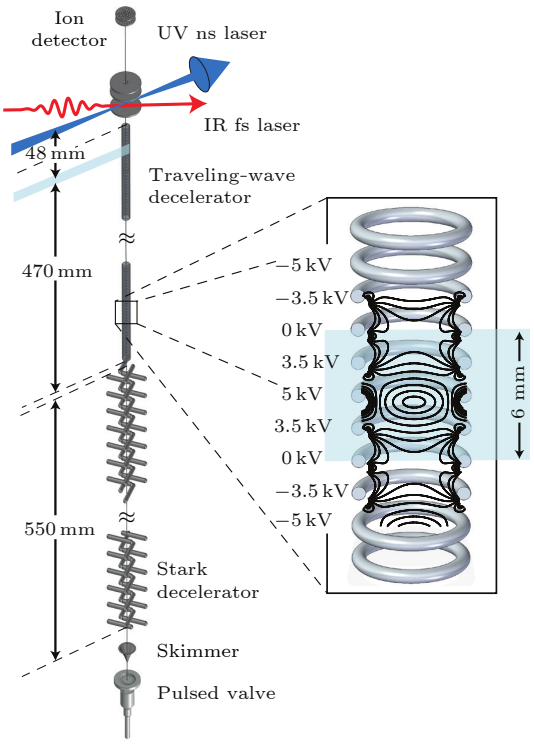

Fig. 1. Schematic view of the vertical molecular beam machine. A beam of ammonia molecules is decelerated and/or trapped using a combination of a Stark decelerator and a traveling wave decelerator. For the bunching experiments, voltages are applied to deliver a traveling potential that moves along with the molecules over a short distance (~15 mm) when the molecules are near the end of the traveling wave decelerator. This distance is indicated with the blue box. The inset shows the electric field magnitude inside the traveling wave decelerator (in steps of 2.5 kV/cm) with the voltages as indicated.

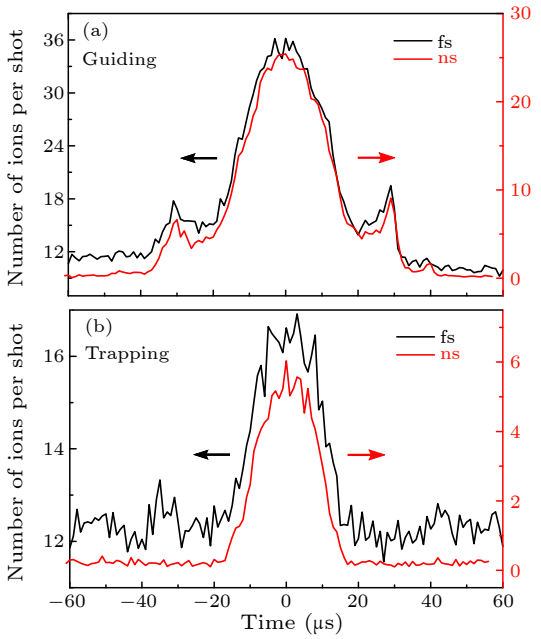

Fig. 2. Observed time-of-flight (TOF) profiles for ammonia molecules when waveforms are applied to the traveling wave decelerator to guide them at 90 m/s (upper panel) or to bring the molecules to a standstill in the middle of the decelerator, trap the molecules for 50 ms, and then accelerate them back to 90 m/s (lower panel). The black curves show the signal obtained using the fs laser (left axes) while the red curves show the signal obtained using the ns laser (right axes).

Figure 2 shows the observed time-of-flight (TOF) profiles for ammonia (NH_3) molecules when waveforms are applied to the traveling wave decelerator to guide molecules at a constant velocity of 90 m/s (upper panel) or to bring the molecules to a standstill in the middle of the decelerator, trap the molecules for 50 ms, and then accelerate them back to their initial velocity and finally detect them (lower panel). The horizontal axis represents the time delay between the arrivals of laser and molecular beam, and time zero is the expected arrival time of the molecules. The black and red curves correspond to the ion signal obtained using the fs and ns lasers, respectively. In both cases, the measured currents are converted to the number of detected ions per shot. To do this, we have performed measurements at very low signal by reducing either the laser power or the molecular beam density. When the MCP voltage is set at 1800 V, the detection of a single ion is correspondingly estimated to be 0.7 units of the measuring program. The ion signal as a function of the MCP voltage is measured and it is found that the signal is approximately doubled when the MCP voltage is increased by 100 V. As observed, the number of detected ions using the fs laser (left axis) is comparable to that obtained with the ns laser (right axis), however, the background for the signal of the fs laser is much larger. This background arises from the thermalized ammonia molecules in the vacuum chamber. As only a small fraction of these thermalized molecules are in the $J = 1$, $K = 1$ state, the observed background for the resonant detection scheme is much smaller. In the previous experiments, we have shown that the background can be effectively suppressed using velocity map imaging.[22] Note that the signal for the guided

NH_3 molecules is a factor of 8 smaller than obtained in earlier experiments with ND_3. This is attributed to the smaller Stark shift of NH_3 and to the increased distance from the detection zone in these experiments. We observe a significant decrease in signal from guiding to trapping, mostly due to poor phase-space matching for NH_3 between the Stark decelerator and the traveling wave decelerator. We expect to improve this by appropriately adjusting the voltages either when the molecules enter the traveling decelerator or once they are trapped. By measuring the ion yield as a function of the energy of the fs pulses, the peak density of the guided and trapped beam is determined to be $2 \times 10^7\,\mathrm{cm}^{-3}$ and $5 \times 10^6\,\mathrm{cm}^{-3}$, respectively.

One motivation of our work is the hope to increase the number of molecules that are being detected to increase the precision of spectroscopic studies on cold molecules.[23,24] With the available intensities, the observed numbers of ions for the fs and ns detection schemes are comparable. Since the detection scheme based on an fs laser suffers from a much greater background noise, it seems advantageous to use the ns laser for experiments with ammonia. However, from inspection of the profile of the multi-mode ns laser beam, we suspect that the detection volume of the ns laser is substantially larger than that of the fs laser. Since in the planned spectroscopic experiments, we use very cold samples that are focused to a very small volume, the fs laser might still be effective.[15,24] To investigate this, we have performed experiments where ammonia molecules are focused to a very small bunch, i.e., so small that it becomes comparable to the size of the laser focus. The applied bunching scheme is similar to that used by Crompvoets *et al.*[25] and Heiner *et al.*[26]

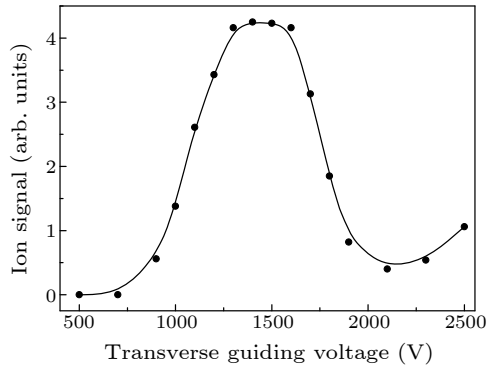

Fig. 3. Ion signal for the ns detection scheme as a function of the voltage used for transversely guiding ammonia molecules through the traveling wave decelerator. In this measurement, the molecules travel at a speed of 150 m/s and the bunching pulse is applied over a length of 13 mm.

In the bunching experiments, we use the conventional Stark decelerator to decelerate molecules to 150 m/s, but now, rather than switching on the traveling potential immediately, we let the molecules expand in the longitudinal direction for most of the length of the traveling wave decelerator before applying the traveling potential. To decrease the spatial spread of the molecules, the voltages applied to the conventional Stark decelerator are reduced to 8.8 kV, thus the molecules leaving the Stark decelerator have spatial and velocity spreads of about $\Delta z = 1$ mm and $\Delta v_z = 5$ m/s, respectively. In free flight, the molecules will disperse; the fast molecules will be ahead of the average while the slow molecules will be behind the average. In phase space this corresponds to an elongated distribution that is tilted with respect to the axes. The applied voltage pulse will accelerate molecules that are behind, while decelerating molecules that are ahead of the packet. In phase space this corresponds to a rotation of the distribution. When the bunching voltages are applied for exactly the right duration, the packet is refocused at the detection zone. In this process the spatial extent is decreased by a factor of L_1/L_2, where L_1 and L_2 are the distances before and after the position of the molecules when the bunching voltages are applied. In our case this corresponds to a factor of about 10, hence the spatial distribution at the detection zone is reduced to below 100 µm. To avoid loss in the transverse direction, we apply constant voltages to the traveling wave decelerator at a reduced amplitude. These voltages focus the molecules in the transverse direction but do not alter the velocity in the longitudinal direction. Figure 3 shows the ion signal measured with the ns detection scheme as a function of this voltage, and we observe a clear maximum when a voltage of around 1.4 kV is applied.

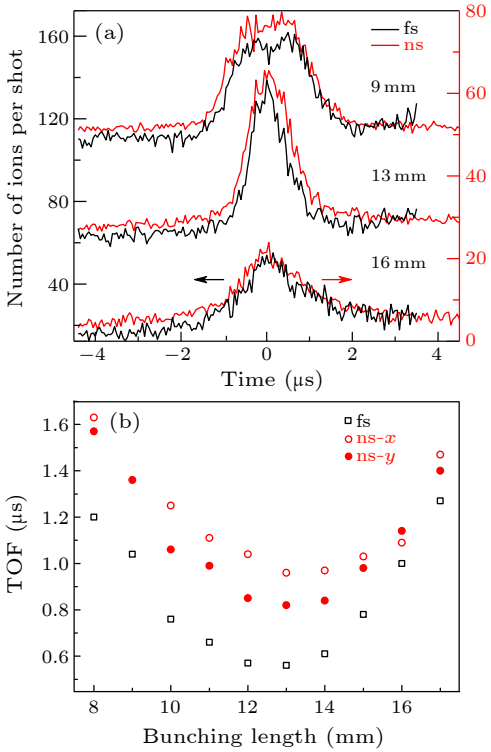

Fig. 4. (a) Observed TOF profiles when waveforms are applied to the traveling wave decelerator to longitudinally focus ammonia molecules in the detection zone. The black curves show the signal obtained using the fs laser (left axis) while the red curves show the signal obtained using the ns laser (right axis). The traveling wave is applied for 9 mm, 13 mm and 16 mm, for the upper, middle and lower curves, respectively. (b) FWHM widths of the observed TOF profiles as a function of the bunching length that the traveling wave decelerator is applied for molecules traveling with a velocity of 150 m/s. Here, ns-x and ns-y denote the cases that ns laser propagates along two mutually orthogonal directions in the transverse plane, respectively.

Figure 4(a) shows a number of observed time-of-flight profiles when the traveling wave decelerator is used to longitudinally focus molecules at the detection zone. The

black curves show the signal obtained using the fs laser (left axis) while the red curves show the signal obtained using the ns laser (right axis). The duration of the pulse applied to the traveling wave decelerator is expressed in terms of length, with the upper, middle and lower curves measured for $L_{\text{bunch}} = 9\,\text{mm}$, 13 mm and 16 mm, respectively. To obtain a measure for the width of the observed TOF profiles, we have subtracted a baseline, integrated and normalized the profiles, and obtained the difference between the times at which 0.25 and 0.75 of the ions are detected. The obtained widths are plotted in Fig. 4(b). The black open squares, red open and solid circles correspond to the measurements using the fs laser, and the ns laser with the laser beam in two orientations denoted by ns-x and ns-y. The minimum width of the TOF profiles is obtained when the bunching pulse is applied over a length of 13 mm. The minimum FWHM obtained with the fs detection scheme is 0.56 µs, corresponding to a spatial spread of 84 µm. Normally the TOF is determined by both the spatial and velocity spreads of the molecules. Under our experimental conditions, the longitudinal spread of the molecules is dominated by the molecular spatial spread induced by the bunching parameters. The width of the detection volume is estimated to be about 80 µm, which suggests that the observed width mainly reflects the diameter of the fs laser beam. As observed in Fig. 4(b) the minimum FWHM obtained with the ns laser is slightly, but significantly, larger than that measured with the fs laser. From this, we conclude that the detection volume for the ns laser has diameters of 140 and 120 µm in the x and y directions, respectively. This conclusion is consistent with the fact that the fs and ns signals for guided and trapped molecules shown in Fig. 2 are similar, while for bunched molecules the signal obtained with the fs laser is almost 2 times larger. The detection volume of the ns laser detection scheme is found to be only 1.5 to 2 times larger. This was slightly surprising to us because of previous measurements that the radius of the detection volume of the ns would be significantly larger.

In conclusion, we use nonresonant multiphoton ionization with an fs laser to detect Stark decelerated ammonia molecules, which provides a general detection method of Stark decelerated molecules. The background can be effectively eliminated by using the VMI technique, and the well-defined detection volume allows an accurate determination of the density of cold molecules. By comparing it to the conventional detection method that employs resonant multiphoton ionization by UV laser light from an ns dye laser, we find that the observed numbers of ions per shot for both schemes are similar at the intensities of the fs and ns lasers available to us. It should be pointed out that in the current experiments we use only 1 out of every 100 pulses from the fs laser system, i.e., the experiment runs at 10 Hz while the fs laser runs at 1 kHz. The signal can be increased by amplifying the fs pulses at a 10 Hz rate using an external amplifier similar to that of Witte *et al.*[27] (increasing the intensity of the ns laser with a similar factor is unfeasible). Another option would be to detect the molecules inside the trap (as was carried out in the previous experiments[13,28]), by lowering the voltages applied to the trap for a short ($< 20\,\mu\text{s}$) duration of time. Under these conditions, the fs laser scheme potentially gives 100 times more signal than the currently used detection scheme.

Acknowledgments. This work was supported by the National Key Research and Development Program of China (Grant No. 2019YFA0307704), the National Natural Science Foundation of China (Grant Nos. 11974425 and 11974426).

References

[1] van de Meerakker S Y T, Bethlem H L, Vanhaecke N, and Meijer G 2012 *Chem. Rev.* **112** 4828
[2] Bethlem H L, Berden G, van Roij A J A, Crompvoets F M H, and Meijer G 2000 *Phys. Rev. Lett.* **84** 5744
[3] Cheng C, van der Poel A P P, Jansen P, Quintero-Pérez M, Wall T E, Ubachs W, and Bethlem H L 2016 *Phys. Rev. Lett.* **117** 253201
[4] Wang Q, Hou S, Xu L, and Yin J 2016 *Phys. Chem. Chem. Phys.* **18** 5432
[5] Du M, Zhang D, and Ding D 2021 *Chin. Phys. Lett.* **38** 123201
[6] de Jongh T, Besemer M, Quan S, Karman T, van der Avoird A, Groenenboom G C, and van der Meerakker S 2020 *Science* **368** 626
[7] Brabec T and Krausz F 2000 *Rev. Mod. Phys.* **72** 545
[8] Posthumus J 2004 *Rep. Prog. Phys.* **67** 623
[9] Backus S, Durfee I C G, Murnane M M, and Kapteyn H C 1998 *Rev. Sci. Instrum.* **69** 1207
[10] Corkum P B 1993 *Phys. Rev. Lett.* **71** 1994
[11] Hankin S, Villeneuve D, Corkum P, and Rayner D 2001 *Phys. Rev. A* **64** 013405
[12] Meng C, van der Poel A P P, Cheng C, and Bethlem H L 2015 *Phys. Rev. A* **92** 023404
[13] Bethlem H L, Crompvoets F M H, Jongma R T, van de Meerakker S Y T, and Meijer G 2002 *Phys. Rev. A* **65** 053416
[14] Ashfold M, Langford S, Morgan R, Orr-Ewing A, Western C, Scheper C, and De Lange C 1998 *Eur. Phys. J. D* **4** 189
[15] Quintero-Pérez M, Wall T E, Hoekstra S, and Bethlem H L 2014 *J. Mol. Spectrosc.* **300** 112
[16] Quintero-Pérez M, Jansen P, Wall T E, van den Berg J E, Hoekstra S, and Bethlem H L 2013 *Phys. Rev. Lett.* **110** 133003
[17] Jansen P, Quintero-Pérez M, Wall T E, van den Berg J E, Hoekstra S, and Bethlem H L 2013 *Phys. Rev. A* **88** 043424
[18] Osterwalder A, Meek S A, Hammer G, Haak H, and Meijer G 2010 *Phys. Rev. A* **81** 051401
[19] Meek S A, Parsons M F, Heyne G, Platschkowski V, Haak H, Meijer G, and Osterwalder A 2011 *Rev. Sci. Instrum.* **82** 093108
[20] Eppink A T and Parker D H 1997 *Rev. Sci. Instrum.* **68** 3477
[21] Janssen M, Parker D H, Sitz G O, Stolte S, and Chandler D W 1991 *J. Phys. Chem.* **95** 8007
[22] Quintero-Pérez M, Jansen P, and Bethlem H L 2012 *Phys. Chem. Chem. Phys.* **14** 9630
[23] van Veldhoven J, Küpper J, Bethlem H L, Sartakov B, van Roij A J A, and Meijer G 2004 *Eur. Phys. J. D* **31** 337
[24] Bethlem H L, Kajita M, Sartakov B, Meijer G, and Ubachs W 2008 *Eur. Phys. J. Spec. Top.* **163** 55
[25] Crompvoets F M H, Jongma R T, Bethlem H L, van Roij A J A, and Meijer G 2002 *Phys. Rev. Lett.* **89** 093004
[26] Heiner C E, Bethlem H L, and Meijer G 2006 *Phys. Chem. Chem. Phys.* **8** 2666
[27] Witte S, Zinkstok R T, Wolf A, Hogervorst W, Ubachs W, and Eikema K S 2006 *Opt. Express* **14** 8168
[28] van Veldhoven J, Bethlem H L, and Meijer G 2005 *Phys. Rev. Lett.* **94** 083001